The reliability of AlGaN/GaN high electron mobility transistors under step-electrical stresses*

Ma Xiao-Hua(马晓华)[a)b)], Jiao Ying(焦 颖)[a)], Ma Ping(马 平)[a)],
He Qiang(贺 强)[a)], Ma Ji-Gang(马骥刚)[a)], Zhang Kai(张 凯)[b)],
Zhang Hui-Long(张会龙)[a)], Zhang Jin-Cheng(张进成)[b)], and Hao Yue(郝 跃)[b)]

[a)] *School of Technical Physics, Xidian University, Xi'an* 710071, *China*

[b)] *Key Laboratory for Wide Band-Gap Semiconductor Materials and Devices, School of Microelectronics, Xidian University, Xi'an* 710071, *China*

(Received 26 May 2011; revised manuscript received 20 July 2011)

In spite of their extraordinary performance, AlGaN/GaN high electron mobility transistors (HEMTs) still lack solid reliability. Devices under accelerated DC stress tests (off-state, $V_{\rm DS} = 0$ state, and on-state step-stress) are investigated to help us identify the degradation mechanisms of the AlGaN/GaN HEMTs. All our findings are consistent with the degradation mechanism based on crystallographic-defect formation due to the inverse piezoelectric effects in Ref. [1] (Joh J and del Alamo J A 2006 *IEEE IDEM Tech. Digest* p. 415). However, under the on-state condition, the devices are suffering from both inverse piezoelectric effects and hot electron effects, and so to improve the reliability of the devices both effects should be taken into consideration.

Keywords: inverse piezoelectric effects, degradation mechanisms, hot electron effects, DC electrical step stresses, AlGaN/GaN HEMTs, reliability

PACS: 73.40.Kp, 73.61.Ey, 78.30.Fs **DOI:** 10.1088/1674-1056/20/12/127305

1. Introduction

Due to their high voltage handling ability, AlGaN/GaN high electron mobility transistors (HEMTs) provide great promise for switching and RF power applications, as in Refs. [2], [3], and [4]. The greatest impediment preventing wide deployment of the devices today is their limited electrical reliability.[5] At present, there is a lack of sufficient understanding about the fundamental mechanisms that limit reliability. The prevailing hypothesis is hot-electron-induced trap formation.[6−8] The electrical degradation mechanisms of AlGaN/GaN HEMTs are studied in this paper, and some suggestions are also given to improve their reliability.

2. Device and fabrication

The AlGaN/GaN HEMT in this work is grown on (0001) sapphire substrate using metal-organic chemical vapour deposition (as shown in Fig. 1). The heterojunction consists of an AlN nucleation layer, a 1.3-μm thick GaN buffer, a 1-nm thick AlN interlayer, and a 22 nm thick $Al_{0.35}Ga_{0.65}N$ barrier layer with a 1 nm thick GaN cap layer. None of the layers are intentionally doped. The conduction band discontinuity between AlGaN and GaN confines the two-dimensional electron gas at the channel–barrier interface. Gate patterns are made by optical lithography with $L_{\rm g} = 0.8$ μm and $W_{\rm g} = 50$ μm, and both a T-shape gate field plate and a source field plate are incorporated to mitigate the peak electric field in the structure. The gate to source spacing $L_{\rm gs}$ is 0.7 μm, whereas the gate to drain spacing $L_{\rm gd}$ is 2.5 μm. Mesa isolation is performed by reactive ion etching with Cl_2. Ohmic contacts are formed by rapid thermal annealing of the Ti/Al/Ni/Au multilayer at 850 °C for 30 s in N_2 ambience. The cross section of the AlGaN/GaN HEMT used in this study is shown in Fig. 1.

*Project supported by the National Basic Research Program of China (Grant No. 2011CBA00600), the National Natural Science Foundation of China (Grant No. 61106106), and the Fundamental Research Funds for the Central Universities (Grant No. K50510250006).

†Corresponding author. E-mail: xhma@xidian.edu.cn

© 2011 Chinese Physical Society and IOP Publishing Ltd

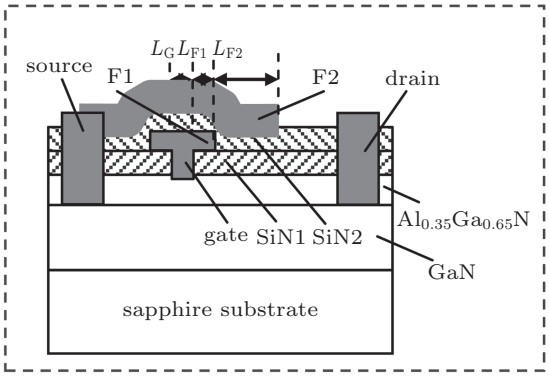


Fig. 1. Cross section of the AlGaN/GaN HEMT.

3. Experiment and discussion

A typical device performs $I_{\rm dmax}$ of 0.81 A/mm and $V_{\rm T}$ of −3.6 V. We electrically stressed the device in the DC field at room temperature. During stress, we measured several device parameters using a benign characterization suite.

The characterization suite involves a benign set of measurements that allows us to monitor the device characteristics during the experiments. In our approach, the electrical stress is interrupted at predefined intervals, and the characterization suite performs a variety of measurements to extract figures of merit that characterize the device. Finally, the stress conditions are resumed. We repeat this cycle at a certain frequency until the end of the test. The monitored figures of merit are given in Table 1. The stress scheme used in this study is shown in Fig. 2.

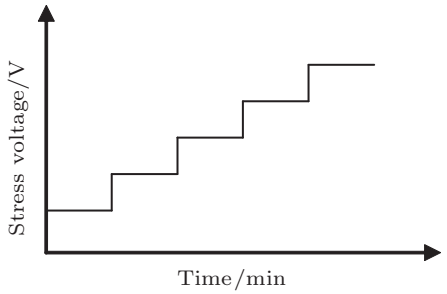


Fig. 2. The stress scheme used in the study.

Table 1. Device parameters monitored during characterization.

Parameters	Definition
$I_{\rm gOFF}$	Leakage current. Measured at $V_{\rm GS} = -10$ V and $V_{\rm DS} = 0.1$ V.
$I_{\rm dmax}$	Maximum drain current. Measured at $V_{\rm GS} = 2$ V and $V_{\rm DS} = 8$ V.
$R_{\rm d}$	Drain resistance. Measured as $V_{\rm DS}/I_{\rm DS}$ when $I_{\rm G} = -I_{\rm D} = 20$ mA/mm (that is, $I_{\rm s} = 0$).
$R_{\rm s}$	Measured as $V_{\rm DS}/I_{\rm DS}$ when $I_{\rm G} = 20$ mA/mm and $I_{\rm D} = 0$ (that is, $I_{\rm s} = -I_{\rm G}$).
$V_{\rm T}$	Defined as $V_{\rm T} = V_{\rm GS} - 0.5V_{\rm DS}$ when $I_{\rm D} = 1$ mA/mm and $V_{\rm DS} = 10$ V.

First, we carry out step-stress experiments in the off-state. This condition is interesting in that no current flows through the channel, and thus the influence of hot electrons is supposed to be eliminated. In a typical experiment, $V_{\rm ds}$ is varied from 5 V to 100 V in 5 V steps with a constant $V_{\rm gs}$ of −8 V. The device is stressed for 10 min at each voltage step. Figure 3 shows the changes in $I_{\rm dmax}$, $I_{\rm gOFF}$, stress gate current $I_{\rm gstress}$, stress drain current $I_{\rm dstress}$, stress source current $I_{\rm sstress}$, $R_{\rm s}$, $R_{\rm d}$, and $V_{\rm T}$ as the stress experiment proceeds. As can be seen, there are several interesting points in this figure. Shown in Fig. 3(a) are two significant points of voltage: 38 and 73 V. Hence we denote the voltage where $I_{\rm gOFF}$ increases suddenly as a critical voltage for the gate leakage current degradation of $V_{\rm crit}$ (73 V). This observation is very similar to the result in Refs. [9] and [10], where such an increase in current degradation is attributed to the inverse piezoelectric effect in the AlGaN/GaN system. We refer to the voltage where $I_{\rm gOFF}$ stops decreasing as V_1 (38 V), which is not found in the experiments in Ref. [7]. Figure 3(b) shows the voltage evolution of $I_{\rm dstress}$, $I_{\rm gstress}$, and $I_{\rm sstress}$ during this experiment. Both $I_{\rm dstress}$ and $I_{\rm gstress}$ exhibit a sharp rise around the same critical voltage denoted in Fig. 3(a), while $I_{\rm sstress}$ presents a negligible change. This phenomenon implies that degradation takes place in the gate to drain region. On the other hand, $R_{\rm s}$ and $R_{\rm d}$, described in Fig. 3(c), show negligible variation, which is a little different from the result in Ref. [9], where $R_{\rm d}$ rises sharply around the critical voltage. In Fig. 3(d) $V_{\rm T}$ continues a positive drift until $V_{\rm dg}$ reaches V_1, then it changes slightly until $V_{\rm dg}$ reaches $V_{\rm crit}$, where $V_{\rm T}$ starts to drift negatively. This is because in off-state step stress, electrons injected from the gate or channel may be trapped in the defects in the fresh device, hence the decrease in $I_{\rm gOFF}$ and $I_{\rm dmax}$, and the apparent plain results from the fulfilling of all the defects. However, when the step stress voltage $V_{\rm dg}$ exceeds $V_{\rm crit}$, new lattice defects acting as electron traps will be produced due to the inverse piezoelectric effect in the AlGaN/GaN system. Electrons moving

between these traps form a leakage path between the gate and the drain. As a result, $I_{\rm gOFF}$, $I_{\rm dstress}$, and $I_{\rm gstress}$ rise sharply, and $V_{\rm T}$ drifts negatively. Although $I_{\rm dmax}$ remains unchanged, which may be due to the GaN cap layer, the mechanism still needs to be further researched.

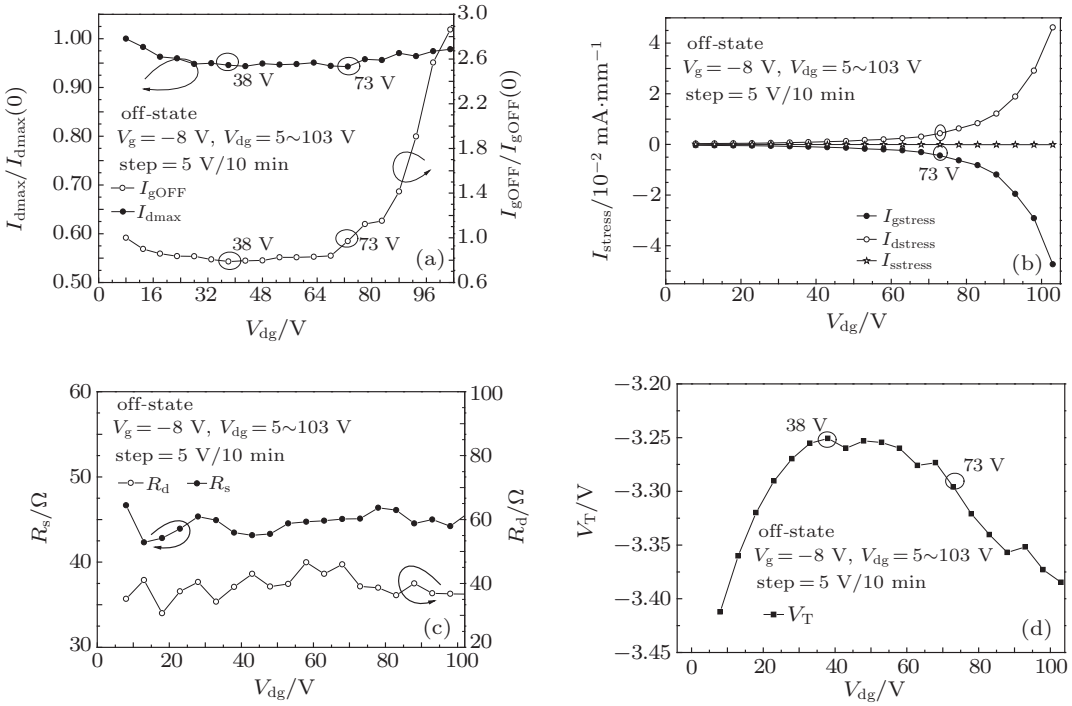


Fig. 3. Changes in (a) normalized $I_{\rm dmax}$ and $I_{\rm gOFF}$, (b) $I_{\rm gstress}$, $I_{\rm dstress}$ and $I_{\rm sstress}$, (c) $R_{\rm s}$ and $R_{\rm d}$, and (d) $V_{\rm T}$ in off-state step-stress experiments.

Then we carry out step-stress experiments at $V_{\rm DS} = 0$, where the gate voltage is held at negative values (from -5 to -55 V, by 1 V per minute) as the drain to source voltage is kept at 0 V. This stress scheme is designed to stress both the drain and source sides of the gate because the same voltage difference between gate–source and gate–drain terminals produces the high electric field on both sides of the gate. The reverse current flowing through the gate is composed of the current coming from the drain and the source. First, in Fig. 4(a), we observe an almost two orders of magnitude increase in gate leakage current beyond $V_{\rm dg} = -53$ V (the limit current is 100 mA·mm^{-1}, so beyond $V_{\rm crit}$, $I_{\rm gOFF}$ keeps constant). Hence we denote the voltage where $I_{\rm gOFF}$ increases by several orders of magnitude as a critical voltage for gate leakage current degradation, $V_{\rm crit}$. This result is very similar to that in Ref. [7], where such an increase in current degradation was attributed to the inverse piezoelectric effect in the AlGaN/GaN system. Also, there is a sudden decrease in $I_{\rm dmax}$ beyond the critical voltage $V_{\rm crit}$. The triggering effect of this mechanism is the vertical fields due to the voltage applied on the gate. Since the fields are more or less symmetrical on both sides of the gate, the impact of stress on the drain is comparable to that on the source side of the device. It is important to note that none of the effects can be attributed to the current or temperature since the channel is off at all applied voltages. In Fig. 4(b) we observe that before critical voltage, $V_{\rm crit}$, $I_{\rm gstress}$, and $I_{\rm sstress}$ increase slowly, while $I_{\rm dstress}$ remains unchanged. However, beyond critical voltage, $V_{\rm crit}$, $I_{\rm gstress}$, and $I_{\rm sstress}$ increase by two orders of magnitude,while $I_{\rm dstress}$ increases by one order of magnitude. This is a little different from Ref. [9], where $I_{\rm gstress}$ and $I_{\rm dstress}$ have a sharp rise and $I_{\rm sstress}$ remains unchanged. This is because in Ref. [9], $L_{\rm gs}$ and $L_{\rm gd}$ are the same, while in this experiment $L_{\rm gs}$ is 0.7 μm and $L_{\rm gd}$ is 2.5 μm. Hence the source side experiences harder conditions and results in a sharp rise in $I_{\rm sstress}$. In Fig. 4(c), while sweep voltage reaches critical voltage, $R_{\rm s}$ starts to decrease sharply and $R_{\rm d}$ starts to increase sharply. We consider this phenomenon as follows: shallow level defects formed in the source to gate region help electrons flow through, which results in a decrease in $R_{\rm s}$. On the other hand, due to the inverse piezoelectric effect, lattice defects such as point defects or line defects formed in the gate to drain region will capture electrons, leading to an increase in

$R_{\rm d}$. However, more detailed reasons need to be researched further. In Fig. 4(d), $V_{\rm T}$ undergoes a similar change to that shown in Fig. 3(d). We also find that $V_{\rm crit}$ under the $V_{\rm DS} = 0$ state is smaller than that under the off-state. This can be explained by the impact of the strain field produced from the source side of the device. As $V_{\rm sg}$ increases, the strain field at the source side of the gate edge increases, and the total elastic-energy density under the gate increases, resulting in a lower $V_{\rm crit}$.

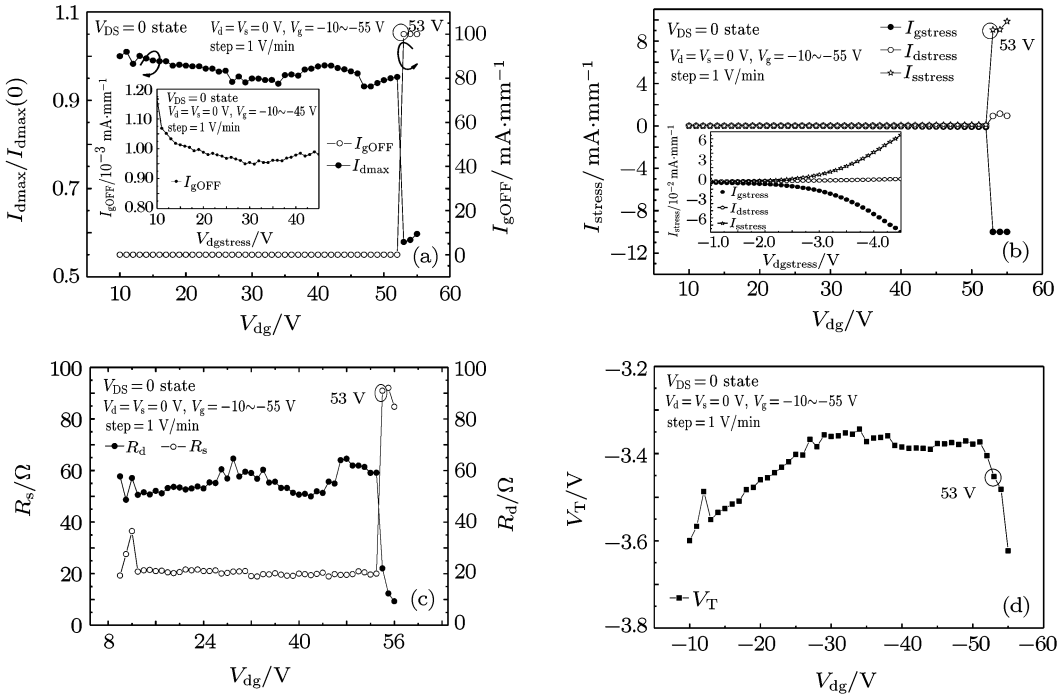


Fig. 4. Changes in (a) normalized $I_{\rm dmax}$ and $I_{\rm gOFF}$, (b) $I_{\rm gstress}$, $I_{\rm dstress}$, and $I_{\rm sstress}$, (c) $R_{\rm s}$ and $R_{\rm d}$, and (d) $V_{\rm T}$ in $V_{\rm DS} = 0$ state step-stress experiments.

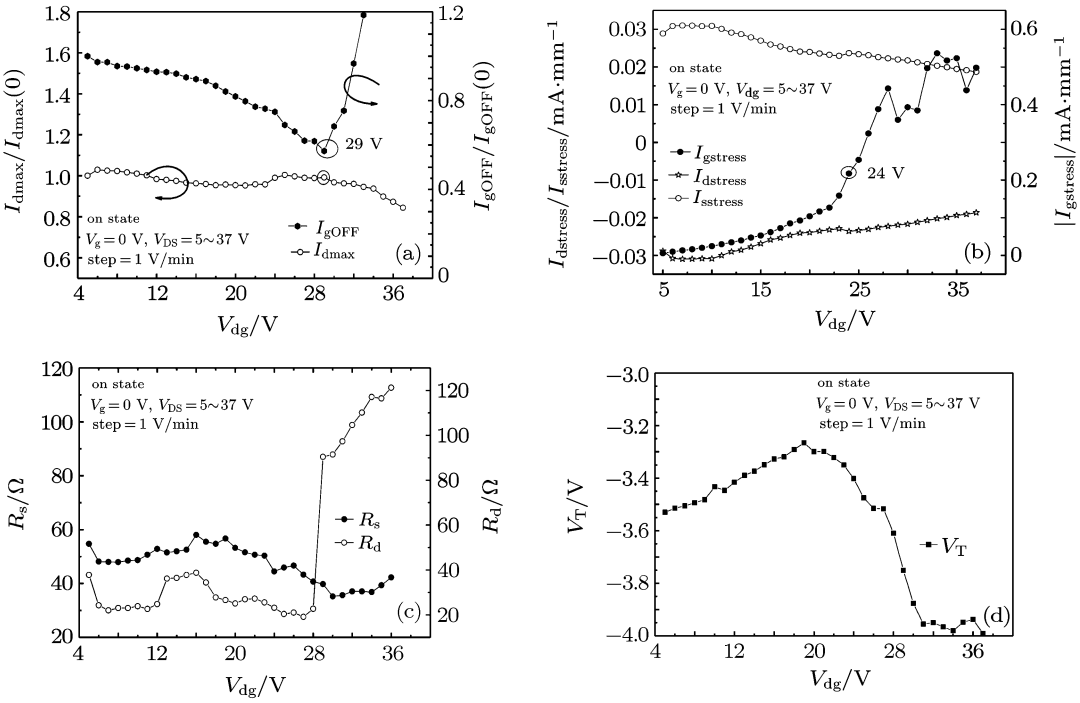


Fig. 5. Changes in (a) normalized $I_{\rm dmax}$ and $I_{\rm gOFF}$, (b) $I_{\rm gstress}$, $I_{\rm dstress}$, and $I_{\rm sstress}$, (c) $R_{\rm s}$ and $R_{\rm d}$, and (d) $V_{\rm T}$ in on-state step-stress experiments.

Finally, we carry out an on-state step-stress experiment, in which $V_{\rm dg}$ is stressed from 5 to 37 V by 1 V per minute, while $V_{\rm g}$ is kept at 0 V. The results of this experiment are shown in Fig. 5. In Fig. 5(a), we find that $I_{\rm gOFF}$ has the same tendency as that shown in Fig. 3(a) or Fig. 4(a), except that $I_{\rm gOFF}$ decreases more than that under the off-state and $V_{\rm DS} = 0$ conditions. This is because large quantities of electrons in the channel under the on-state are trapped by defects existing in the fresh device, resulting in more of a decrease in $I_{\rm gOFF}$. Also we find that $I_{\rm dmax}$ begins to decrease beyond $V_{\rm crit}$. However, unlike a sudden decrease in the $V_{\rm DS} = 0$ state, it decreases slowly in this experiment. We consider that this change in $I_{\rm dmax}$ may be due to the hot electron effect. In Fig. 5(b), $I_{\rm gstress}$ keeps increasing, while $I_{\rm dstress}$ and $I_{\rm dstress}$ change a little. This fact confirms the existence of the inverse piezoelectric effect. In Fig. 5(c), we find that $R_{\rm s}$ changes a little, while $R_{\rm d}$ has a sharp rise beyond $V_{\rm crit}$. In Fig. 5(d), $V_{\rm T}$ has the same tendency as that in Fig. 3(d) or Fig. 4(d). We should realize that both the hot electron effect and the inverse piezoelectric effect co-exist in this experiment. We should also pay attention to the fact that the critical voltage $V_{\rm crit}$ here is the smallest among the above three experiments, while the stress voltage $V_{\rm dg}$ is still the smallest. So we can conclude that the hot electron effect may conversely intensify the piezoelectric effects. However, this explanation needs to be verified further.

4. Conclusion

First we discovered that the inverse piezoelectric effect exists in all three experiments, that is to say it exists under all the conditions. So we arrived at the conclusion that the inverse piezoelectric effect is the general degradation mechanism of the AlGaN/GaN HEMTs. Second the degradation typically occurs in the region of the gate to drain even in the $V_{\rm DS} = 0$ state, where the source experiences stringent conditions. Thus mitigating the electric field between the gate and drain may improve the reliability of the AlGaN/GaN HEMTs. Third a GaN cap layer can prevent the degradation of $I_{\rm dmax}$ under off-state conditions, but this seems to have quite limited effects under $V_{\rm DS} = 0$ and on-state conditions. Therefore, a better method is necessary to improve the reliability of $I_{\rm dmax}$. Finally, although devices under on-state conditions suffer the smallest voltage difference $V_{\rm dg}$, they have the lowest critical voltage $V_{\rm crit}$. Thus, despite the inverse piezoelectric effect being the predominant degradation mechanism of the AlGaN/GaN HEMTs, we cannot ignore the influence of the hot electron effect, which may aggravate the inverse piezoelectric effect.

References

[1] Joh J and del Alamo J A 2006 *IEEE IEDM Tech. Digest* December 11–13, 2006, San Francisco, USA p. 415

[2] Meneghesso G, Verzellesi G, Danesin F, Rampazzo F, Zanon F, Tazzoli A, Meneghini M and Zanoni E 2008 *IEEE Trans. Device and Material Reliability* **8** 332

[3] Ma X H, Pan C Y, Yang L Y, Yu H Y, Yang L, Quan S, Wang H, Zhang J C and Hao Y 2011 *Chin. Phys.* B **20** 027304

[4] Ma X H, Ma J G, Yang L Y, He Q, Jiao Y, Ma P and Hao Y 2011 *Chin. Phys.* B **20** 067304

[5] Rongming C, Likun S, Fichtenbaum N, Brown D, Zhen C, Keller S, DenBaars S P and Mishra U K 2008 *IEEE Electron. Dev. Lett.* **29** 974

[6] Sozza A, Dua C, Morvan E, Delage S, Rampazzo F, Tazzoli A, Danesin F, Meneghesso G, Zanoni E, Gurutchet A, Malbert N, Labat N, Grimbert B and de Jaeger J C 2005 *IEEE IEDM Tech. Digest* December 5–7, 2005, San Francisco, USA p. 590

[7] Kim H, Thompson R M, Tilak V, Prunty T R, Shealy J R and Eastman L F 2003 *Electron. Dev. Lett.* **24** 421

[8] Kunii T, Totsuka M, Kamo Y, Yamamoto Y, Takeuchi H, Shimada Y, Shiga T, Minami H, Kitano T, Miyakuni S, Nakatsuka S, Inoue A, Oku T, Nanjo T, Oishi T, Ishikawa T and Matsuda Y 2004 *IEEE CSIC Digest* December 13–15, 2004 San Francisco, USA p. 197

[9] Joh J, Xia L and del Alamo J A 2007 *IEEE IEDM Tech. Digest* December 10–12, 2007, Washington DC, USA p. 385

[10] Joh J and del Alamo J A 2008 *IEEE Electron. Dev. Lett.* **29** 287